Pharmacophore modeling and 3D quantitative structure-activity relationship analysis of febrifugine analogues as potent antimalarial agent

Debanjan Sen,
Tapan Kumar Chatterjee[1]

Bengal Institute of Pharmaceutical
Sciences, Kalyani, Nadia, W.B.
[1]Department of Pharmaceutical
Technologies, Division of Pharmacology,
Jadavpur University, Kolkata, India

J. Adv. Pharm. Tech. Res.

Abstract

Febrifugine and its derivatives are effective against *Plasmodium falciparum*. Using PHASE algorithm, a five-point pharmacophore model with two hydrogen bond acceptor (A), one positively ionizable (P) and two aromatic rings (R), was developed to derive a predictive ligand-based statistically significant 3D-quantitative structure-activity relationship (QSAR) model ($r^2 = 0.972$, SD = 0.3, F = 173.4, $Q^2 = 0.712$, RMSE = 0.3, Person-R = 0.94, and $r^2_{pred} = 0.8$) to explicate the structural attributes crucial for antimalarial activity. The developed pharmacophore model and 3D QSAR model can be a substantial tool for virtual screening and related antimalarial drug discovery research.

Key words: Antimalarial, febrifugine, pharmacophore, PHASE, 3D QSAR

INTRODUCTION

More often than not, the focus of various studies has been to demonstrate antimalarial efficacy *in vitro* for new structural classes or modification of the natural product architecture. Two Chinese medicinal plant *Dicora febrifugia* and *Hydrangea umbellate*[1,2] are the sources of Febrifugine [Figure 1] and Isofebrifugine [Figure 2],[3] which have proved inhibitory action against *Plasmodium falciparum* malaria with novel mechanism of action.[4] Febrifugine contain a 4-quinazolinone ring linked to a 3" hydroxyl piperidine ring with a propyl-2-one chain[5] and compounds with modified side chain attached to the N-3 site of 4-quinazolinone ring posed to be ineffective. The structure-activity relationship (SAR) study revealed that 4-quinazolinone ring, 1" nitrogen atom and 3" hydroxyl group of febrifugine, is imperative

for its remarkable antimalarial property,[6,7] which exhorted ample interest toward febrifugine-based antimalarial drug development. Contrarily, the compounds fabricate unavoidable human toxicity and arduous synthesis. The challenging synthesis inspired scientists to synthesize a large number of febrifugine derivatives, among them *Oshima et al.* (2003) developed a new class of febrifugine analogues with high selectivity and minimal toxicity,[8] antimalarial activity against chloroquine-resistant *P. falciparum* (FCR) strain. A rational approach for the discovery of a pharmaceutically acceptable, economically viable, antimalarial awaits development of a global mechanism of action model for febrifugine and its analogues and/or a predictive quantitative structure-activity relationship (QSAR)-based pharmacophore model. One method of coordinating these strategies is to make use of QSAR models for the rapid prediction and virtual prescreening of antimalarial activity. Our efforts to furnish new iterations of QSAR (Scheme 1) in this area have been chronicled, leading to highly bioactive derivatives of febrifugine. The developed theoretical assumptions revealed a lucid idea for enhanced understanding about SAR of febrifugine and its congeners.
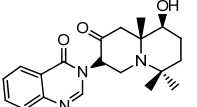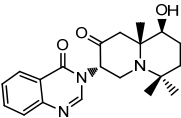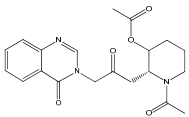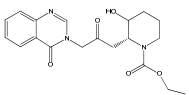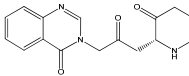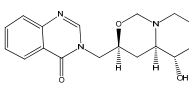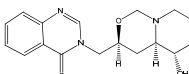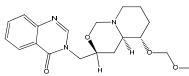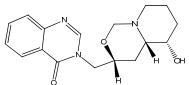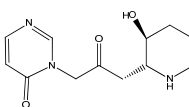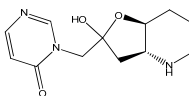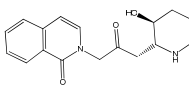
MATERIALS AND METHODS

Datasets and Biological Activity
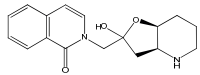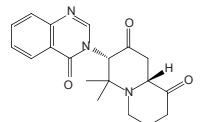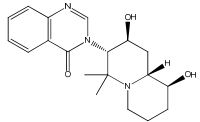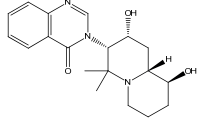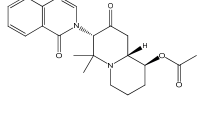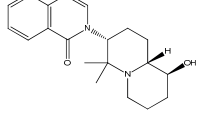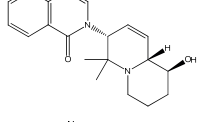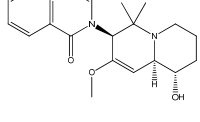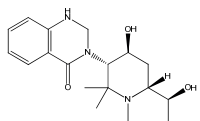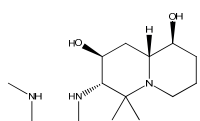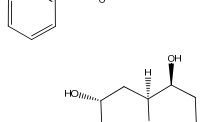
A total of thirty three (33) febrifugine derivatives[8-10] were collected from literature showing *in vitro* activity in terms of EC_{50} value in moles [Table 1] against *P. falciparum* FCR-3 strain.[11] The biological activities considered for the study were converted to pIC_{50} ($-\log EC_{50} + 9$), using

Table 1: Structures of febrifugine derivatives

ID	Structure	Activity[a]	Pred. act[b]
1#		9.796	9.9
2#		8.553	8.72
3		6.04	5.85
4#		5.347	5.17
5		7.699	7.63
6		7.699	8.07
7#		8.432	8.43
8#		8.066	7.94
9#		6.076	6.06
10#		6.222	6.54
11#		7.398	7.33
12#		6.301	6.73

(Continued)

Table 1: Contd/-

ID	Structure	Activity[a]	Pred. act[b]
13#		5.678	5.85
14#		8.721	8.61
15		6.398	7.17
16		6.523	6.75
17#		8.444	8.38
18		6.081	5.72
19#		5.319	5.13
20#		5.886	5.79
21#		6.377	6.33
22#		6.222	6.03
23#		7	7.23

Continued

Table 1: Contd/-

ID	Structure	Activity[a]	Pred. act[b]
24		6.097	6.63
25#		5.469	5.52
26#		6.398	6.36
27#		5.155	5.12
28		7.721	8.21
29#		8.658	8.19
30#		5.18	5.52
31#		7.658	7.06
32#		9.569	9.65
33#		6.824	6.44

#indicates training set ligands rest are test set ligands; [a]Experimental activity pIC_{50} value; [b] Predicted activity

Gaussian statistics to secure more significant Figure for visualizing bioactivity. All the 2D molecular structures were sketched and transformed into 3D structures using ChemDraw Ultra 8.0.
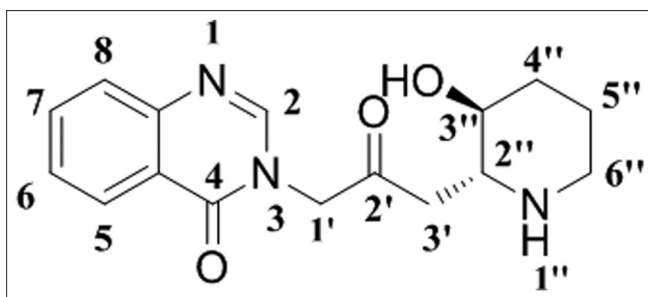
Figure 1: Febrifugine
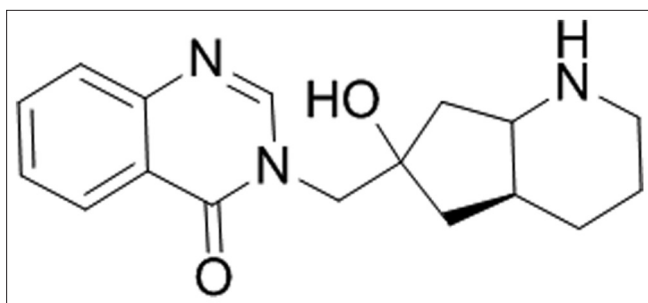
Figure 2: Isofebrifugine
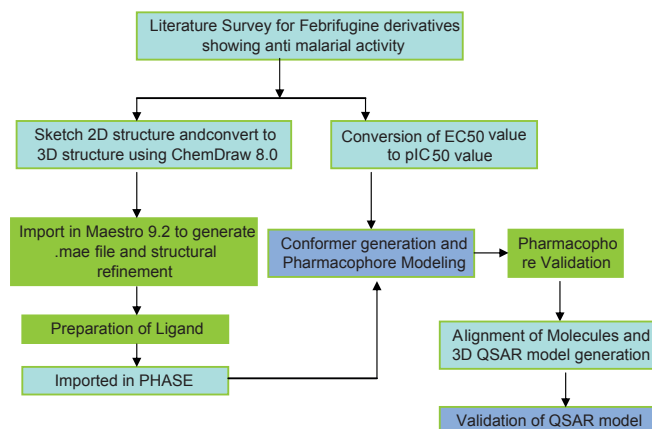
Scheme 1: Graphical representation of Pharmacophore model generation and QSAR analysis

Ligand *Preparation*

Energy minimization was done using OPLS 2005 force field of Ligprep module of Schrodinger Molecular modelling Suite 2011. The pH of ionization of the molecules was taken to be neutral.[12-14] For the development of the pharmacophore model, these ligands were imported in PHASE. Conformation generation is an important step in PHASE algorithm; conformations were generated using ConFigureen taking GB/SA solvent model. About 1 000 conformers were generated per structure ensuring 50 step minimization.[15] The minimized conformers were filtered using a relative energy parameter limitation of 10 kcal/mol and a minimum atom deviation of 1.00 Å. If there was any conformer higher than this limit, or redundant, its incessant disposition was ensured. Thus, the lowest energy non-redundant conformers of a ligand were used

for pharmacophore model development.[16] A couple of conformer was defined as identical if the relative distance between them is below 1.00 Å.[17]

Creating Pharmacophore Sites and Common Pharmacophore Hypothesis Generation

According to the bioactivity, the molecules were divided into actives and inactives, setting the maximum and minimum values in the activity threshold window of PHASE. Pharmacophore sites of a ligand are represented in the 3D space by a set of points. These points coincide with various chemical characteristics with type, location, and directionality, which facilitate non-covalent bonding with the receptor sites. The pharmacophore features like hydrogen bond acceptor (A), hydrogen bond donor (D), hydrophobic/Non-polar group (H), negatively ionizable (N), positively ionizable (P), and aromatic ring (R) were used to create the pharmacophore sites for the energy-calculated ligands. The following features were assigned using SMART queries [Tables 2a,b].[18-20] Tree-based partition algorithm is used by PHASE for detection of common pharmacophore from a set of variants taking maximum tree depth 3. To find common pharmacophore, PHASE algorithm use an exhaustive analysis of k-point pharmacophore match picked from the conformations of a set of active ligands on the basis of inter site distances,[21] and then find all spatial arrangements of pharmacophore features those are common to at least 8 of 10 active ligands. The generated pharmacophores match different set of actives eliminating the chance of its exclusiveness toward a small subset of ligands. The different pharmacophore hypotheses were further examined by using a scoring function, so that it produced the best alignment of the ligands.

Scoring Pharmacophore Hypotheses

The scoring of the pharmacophore hypotheses was done in relation to the information from the active ligands considering various geometric and heuristic factors. The alignment to a reference pharmacophore is considered according to RMSD

Table 2a: Distance (in Å) between the sites

*CPH ID	Site 1	Site 2	Distance
AAPRR.44	A3	A4	4.833
AAPRR.44	A3	P10	5.964
AAPRR.44	A3	R11	3.704
AAPRR.44	A3	R12	2.688
AAPRR.44	A4	P10	3.359
AAPRR.44	A4	R11	6.676
AAPRR.44	A4	R12	4.381
AAPRR.44	P10	R11	7.872
AAPRR.44	P10	R12	6.22
AAPRR.44	R11	R12	2.433

*Common Hypothesis. AAPRR common pharmacophore models were generated with different combination of variants; the results were illustrated in the Table 2a-b.

Table 2b: Angle between the sites

Entry	Site I	Site 2	Site 3	Angle
AAPRR.44	A4	A3	P10	34.3
AAPRR.44	A4	A3	R11	102.1
AAPRR.44	A4	A3	R12	64
AAPRR.44	P10	A3	R11	106.7
AAPRR.44	P10	A3	R12	82.6
AAPRR.44	R11	A3	R12	41
AAPRR.44	A3	A4	P10	91.6
AAPRR.44	A3	A4	R11	32.9
AAPRR.44	A3	A4	R12	33.5
AAPRR.44	P10	A4	R11	97.8
AAPRR.44	P10	A4	R12	106.2
AAPRR.44	R11	A4	R12	8.5
AAPRR.44	A3	P10	A4	54.1
AAPRR.44	A3	P10	R11	26.8
AAPRR.44	A3	P10	R12	25.4
AAPRR.44	A4	P10	R11	57.2
AAPRR.44	A4	P10	R12	42.6
AAPRR.44	R11	P10	R12	14.7
AAPRR.44	A3	R11	A4	45.1
AAPRR.44	A3	R11	P10	46.5
AAPRR.44	A3	R11	R12	46.5
AAPRR.44	A4	R11	P10	25
AAPRR.44	A4	R11	R12	15.5
AAPRR.44	P10	R11	R12	40.3
AAPRR.44	A3	R12	A4	82.6
AAPRR.44	A3	R12	P10	72
AAPRR.44	A3	R12	R11	92.5
AAPRR.44	A4	R12	P10	31.2
AAPRR.44	A4	R12	R11	155.9
AAPRR.44	P10	R12	R11	125

AAPRR common pharmacophore models were generated with different combination of variants; the results were illustrated in the Table 2a-b.

of the site points and the average cosine of the vectors keeping their tolerance 1.2 Å and 0.5, respectively. To get the reference ligand from the most active set, upper 10% was considered for score calculation. For further refinement, volume scoring was performed in order to measure quantitatively of how each non-reference ligand is superimposing with the reference ligand. Here, the cutoff for volume scoring was kept at 1.00 for the non-reference pharmacophores.

3D-Quantitative Structure-Activity Relationship Model Generation

To produce a statistically significant 3D-QSAR model, the first and the foremost requirement is the alignment of ligands; therefore, to execute the QSAR study, a pharmacophore-based alignment was considered. The PHASE algorithm uses a very flexible approach for the development of 3D QSAR model. It considers a rectangular grid of 1 Å grid distance in a 3D space. Thus, it creates cubes of said dimension in the 3D space. The atoms of the molecules which are considered

as overlapping Vander Waal spheres fall inside these cubes depending on the volume of the atomic spheres. These occupied cube spaces are termed as volume bits.[18,22] A volume bit is allocated for each different class of atom that occupies a cube. There are six atom classes, viz. two hydrogen bond acceptor (A), one positively ionizable (P), and two aromatic ring (R) used for classifying the atom characteristics. The total number of volume bits consigned to a specified cube is based on how many training set molecules occupy that cube. A single cube may represent the occupation by one or various atoms or sites, and even those from the same molecule or may be from unlike molecules of the training set. Thus, a molecule may be represented by a binary string concurrent to the occupied cubes, and also the various types of atomic sites that exist in those cubes.

To create an atom-based QSAR model, these volume bits which encode the geometrics and chemical characteristics of the molecule are regarded as independent variables in PLS (Partial Least square) regression analysis.[23] For generating a predictive QSAR model, we have to select six number of PLS factor. The maximum PLS factor that can be taken is N/5, where N is the number of ligands present in the training set.

RESULTS

Pharmacophore Modeling

Several five-point common pharmacophore hypotheses with various combination of site were generated using active molecules. The pharmacophore models were ranked on the basis of alignment to the active compounds; a scoring function and ten pharmacophore hypotheses survived. The "survival" scoring (S) function identifies the best candidate from the generated models and assigns an overall ranking of all the hypotheses. The scoring algorithm includes contributions from the alignment of site points and vectors, volume overlap, selectivity, number of ligands matched, relative conformational energy, and activity. However, the models should also discriminate between active and inactive molecules. If inactive molecule scores well, the hypothesis could be invalid as it does not discriminate between actives and inactives. For the following reason, adjusted survival score S_I (Survival score – Inactive molecule scoring) was calculated by subtracting the inactive score from survival score [Table 3]. On the basis of high S_I score and using a rescoring function (Post-hoc), AAPRR.28, AAPRR.44, AAPRR.67, hypotheses were chosen. By using the test set compounds, the predictive ability of each hypothesis was analyzed. A summary of all pharmacophore-based QSAR model (Model 1-3) with statistical parameters is summarized in Table 4.

A statistically significant valid QSAR model[24] can bring trustworthy results. Considering various statistical parameters such as R^2 (Correlation coefficient), Q^2 (q^2 for the predicted activity), *SD* (Standard deviation), *RMSE* (Root mean square

error), *P* (Significance level of variance ratio), *F*-Statistics, *Pearson-R* (correlation between the predicted and observed activity), a statistically significant QSAR model was generated. To avoid over-fitting of the results, four PLS factor was used.

3D Quantitative Structure-Activity Relationship

From the Table 4, R^2 is greater than 0.900, SD value is lower than 0.35, and F-statistics value is high, which clearly indicate that all these models can describe the SAR properties of all training set molecules. But it is important to select a QSAR model based on its predictive ability. Therefore, we consider a model having high Q^2, and r^2_{pred} value determined by using the formula r^2_{pred} = 1-PRESS/ SSD for further analysis. The Q^2= 0.712 and r^2_{pred}, = 0.84 value of Model-2 is higher than all other models. But the lowest RMSE value and highest Pearson-R value was found in Model-1. Due to impressive and consistent predictive ability of Model-1, it can be termed as best 3D QSAR model of febrifugine derivatives.

DISCUSSION

The special arrangement of features along with their distance present in five featured pharmacophore (AAPRR-44, [Figure 3]) depicted two rings aromatic features, mapped in the 4-quinazolinone ring of highest active as well as reference ligand, 29. The hydrogen bond acceptor feature is mapped to the C=O group at 4th position of 4-quinazolinone ring and on 2′ position of linker chain and positive ionic feature is mapped 1″ NH atom of piperidine ring. This hypothesis was used to align [Figure 4] the dataset and
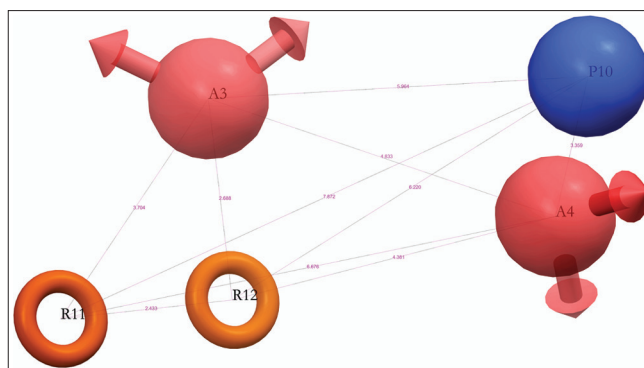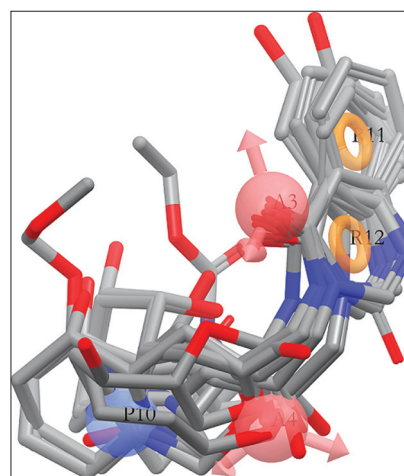

Figure 3: Pharmacophore
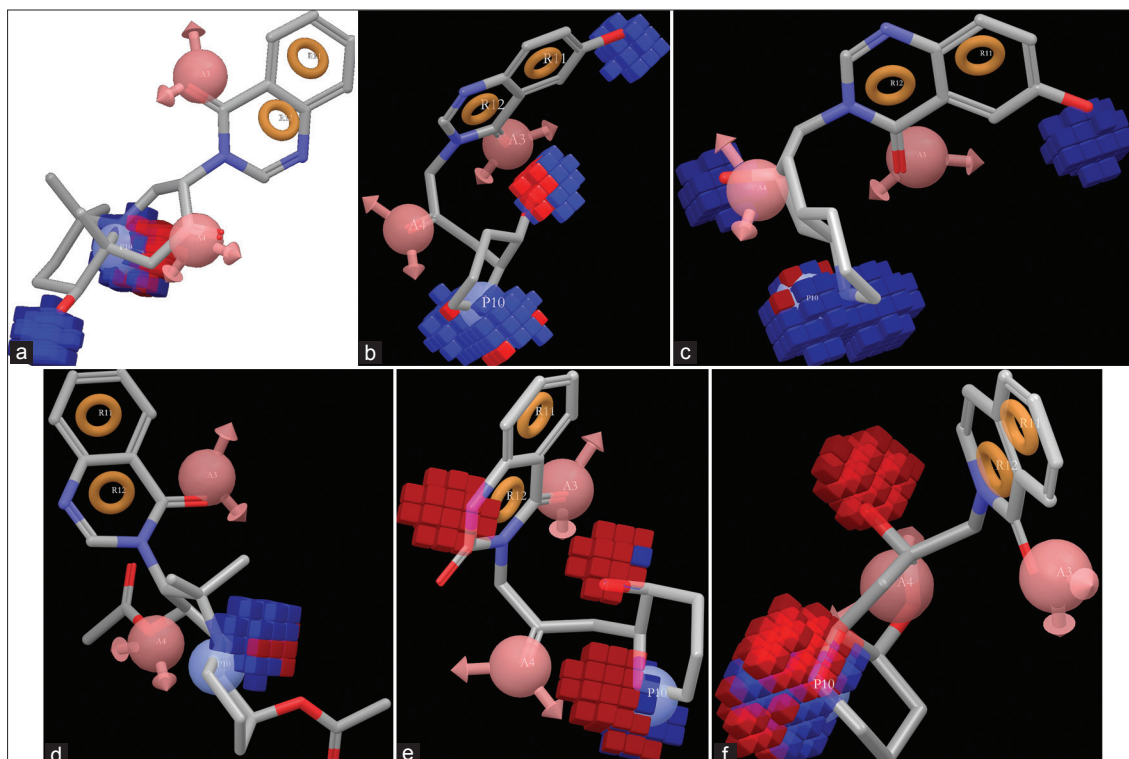

Figure 4: Alignment of molecules_1

Figure 5(a-f): H-Bond donor effect upon Ligand 1

analyze by developing PHASE 3D QSAR model utilizing four PLS factor.

The color maps around the ligands obtained by PHASE QSAR indicate that ligand-based 3D QSAR analysis can define the important features and effects of various substitutions upon febrifugine derivatives for their antimalarial action. It is helpful to recognize important sites which require a certain physicochemical property

for developing potent antimalarials. The blue color region indicates the positive effect and red color region indicates negative effects of particular physicochemical properties. To recognize the PHASE QSAR maps, it is necessary to analyze the pharmacophore-based alignment [Figure 4].

H-Bond Donor
The features of hydrogen bond donor that has been obtained from the QSAR model applied to the most active ligands 1, 29,

Table 3: Phase hypothesis

ID	ID	Survival	Survival-inactive	Post-hoc	Site	Vector	Volume	Selectivity
1	AAPRR.44	2.73	0.936	7.064	0.41	0.851	0.474	2.116
2	AAPRR.28	2.615	0.899	6.968	0.33	0.854	0.455	2.082
3	AAPRR.67	2.611	0.874	6.94	0.3	0.847	0.464	2.089
4	AAPRR.43	2.622	0.848	7.05	0.42	0.819	0.482	2.096
5	AAPRR.27	2.565	0.822	6.894	0.32	0.822	0.423	2.081
6	AAPRR.26	2.603	0.792	6.928	0.32	0.828	0.451	2.067
7	AAPRR.42	2.642	0.791	6.973	0.38	0.8	0.464	2.081
8	AAPRR.25	2.591	0.778	6.924	0.32	0.828	0.447	2.067
9	AAPRR.74	2.554	0.651	6.885	0.25	0.826	0.48	2.112
10	AAPRR.73	2.481	0.614	6.805	0.26	0.762	0.454	2.103
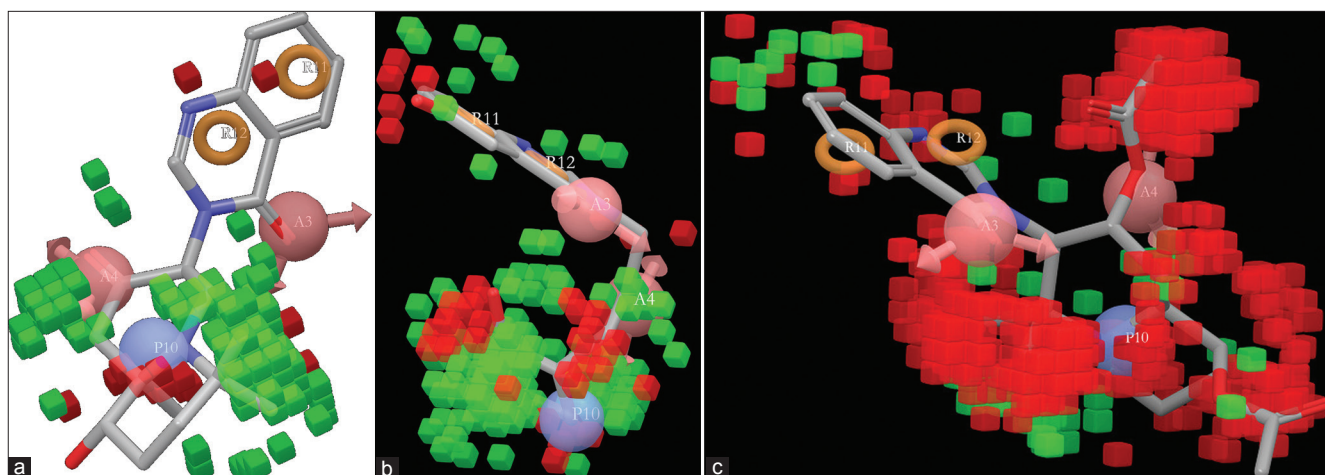
Figure 6(a-c): Effect of hydrophobicity upon ligand 1
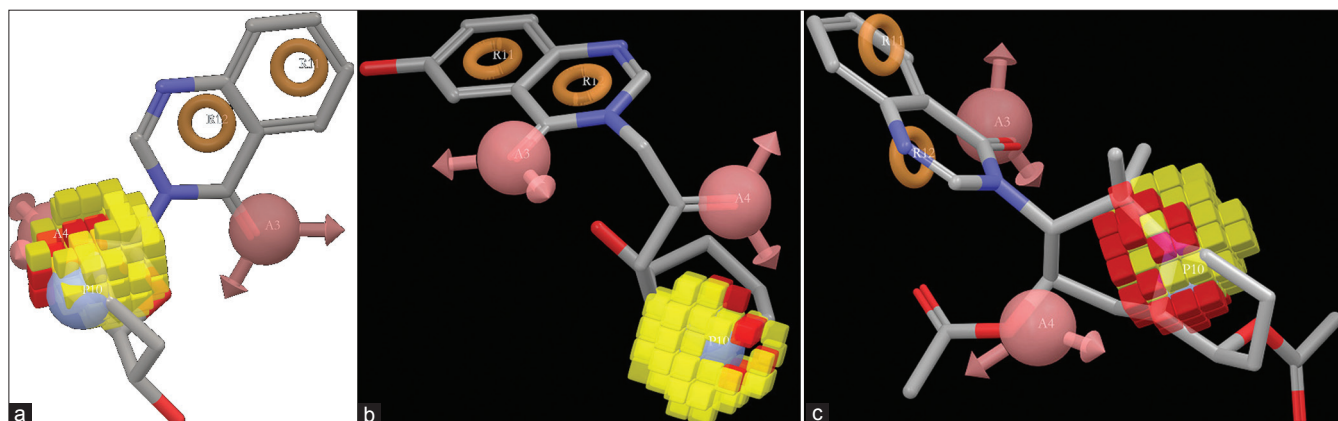
Figure 7(a-c): Effect of positive ionic effect upon ligand 1

Table 4: Summary of the 3D-QSAR model

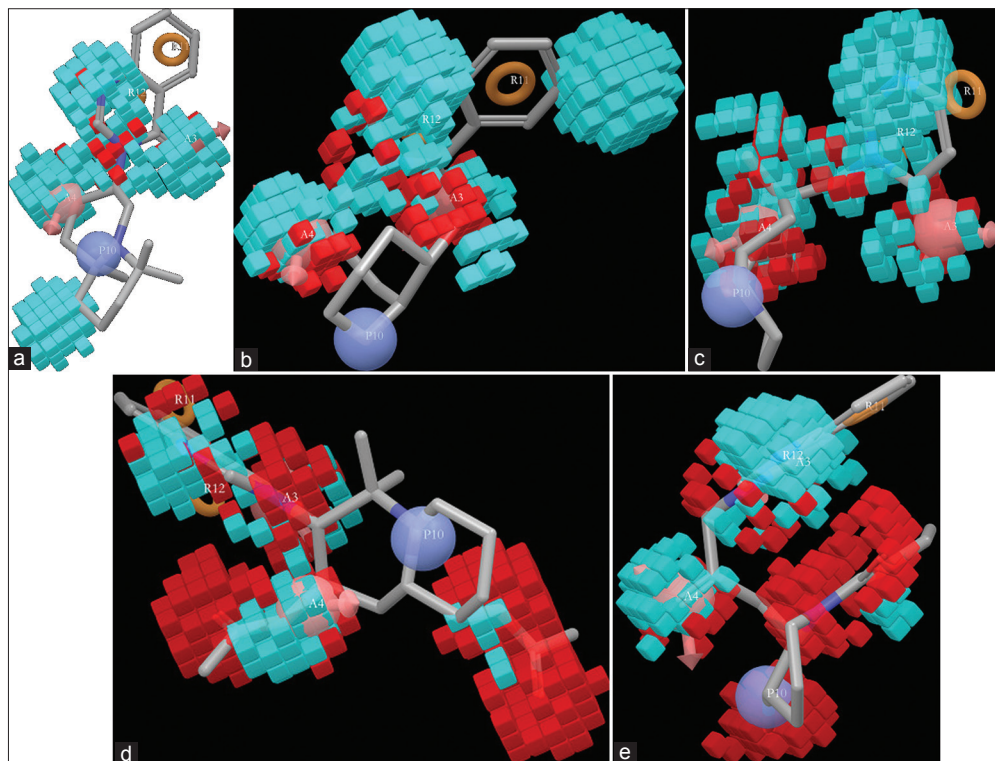| SI no	CPH_ID	SD	R^2	F-Stat	Q^2	Pearson-R	r^2_{pred}
Model-1	AAPRR.28	0.263	0.922	100.2	0.605	0.731	0.76
Model-2	AAPRR.44	0.263	0.972	173.4	0.712	0.943	0.84
Model-3	AAPRR.67	0.361	0.954	136.81	0.594	0.673	0.64

Figure 8(a-c): Effect of electron-withdrawing group

32; less active ligands 27, 30; and moderately active ligand 13 are shown in Figure 5a-f (supplementary data 5b-f). The blue color indicates the favorable and red color indicate unfavorable region of H-Bond donor group for antimalarial activity.

As illustrated in Figure 5a-f, the blue region or H-bond donor favorable region is found around the N-1" atom of piperidine of all molecules, which indicates that this secondary amino ($2°$ NH_2) group is very crucial for biological activity. In the compound 1, 13, and 30, the appearance of red color region along with blue color region where N-1" atom is in *trans* conformation indicates the importance of this particular stereo-isomer on biological activity. There is no red color region that appears around N-1" atom in 29 which is the reference ligand and in 32 where this secondary amino ($2°$ NH_2) group is in *cis* confirmation. Earlier, this fact was specifically established by synthetic chemists. [11] Moreover, this phenomenon indicates the superior predictive ability of our model.

The blue color region around 3" hydroxyl group of piperidine ring of all ligands indicates the importance of this group for

showing biological activity. Appearance of red color region at N-1 position of 4-quinazolinone ring indicates reduction of C=N group of 4-quinazolinone ring which is unfavorable for activity. The 6-hydroxyl group of 4-quinazolinone ring is essential for antimalarial activity and an important feature because it reduce the toxicity which was indicated by blue color region in the active ligands 29, 32, formerly depicted by *in vivo* assay of *Plasmodium berghei* model.

Effect of Hydrophobic/Non-polar *Substitution*
When the QSAR model is applied upon the highest active molecule 1, reference ligand 29, and lowest active ligand 27, the red color region indicate the unfavorable and green color region indicates the favorable hydrophobic/non-polar interaction sites [Figure 6a-c] (supplementary data 6b,c). The green color region around the di-methyl substitution adjacent to N-1" atom indicates favorable position for antimalarial activity. But substitutions at N-1" atom will be unfavorable for activity; this was indicated by the red color region emerging around the aforesaid positions. Bulky substitution at 6-hydroxy group will reduce the biological activity. The bulkier substitution is unfavorable

for biological activity. Substitution with ether groups may reduce antimalarial property.

Positive Ionic Effect

Figure 7a-c (supplementary data 7b-c) discloses the favorable and unfavorable region for positive ionic effects. The yellowish region indicates the positive effect and red color indicate negative effect upon biological activity. In every ligand, yellow color region appears around the N-1″ atom of piperidine ring which indicates that this atom is crucial for biological activity.

Effect of Electron-Withdrawing *Group*

The cyan color around the ligand indicates the addition of electron-withdrawing group that will favor the antimalarial activity and the red color region indicates unfavorable position for substitution with electron-withdrawing groups [Figure 8a-e] (supplementary data 8b-e). The cyan color around the N-1 atom of 4-quinazolinone ring indicates that electron-withdrawing effect is essential for producing antimalarial action. The N-1 atom basically attach with carbon atom by a double bond in the -C=N-C- orientation. Analyzing this feature in ligand **11** which contain substituted pyrimidin ring instead of 4-quinazolinone moiety, it is clear that N-methylene-methane-amine residue is very important for antimalarial action. Moreover, in lowest active ligand 27, the cyan color around the -C=N-C- region indicates its inevitability for biological activity. In the less active ligand 27**,** red colors around the acetylated hydroxyl group indicates that these positions are unfavorable for substitution with electron-withdrawing group. This may reduce the antimalarial property. In the reference ligand 29, substitutions with weak electron-withdrawing group at C-2 atom of quinazolinone ring may increase the biological activity. Substitution at C-2′ position with weak electron-withdrawing group is favorable for showing antimalarial effect. If the N-1″ atom is substituted with electron-withdrawing group, it will reduce the biological activity which is found in ligand 4 which contain ethyl piperidine-1-carboxylate moiety.

CONCLUSION

The study represents the pharmacophoric features of febrifugine analogues as a potential antimalarial agent. It depicts a five-point pharmacophore with two hydrogen bond acceptors (A), one positive ionic effect producing group (P), and two aromatic rings (R). A 3D-QSAR model with good statistical significance and predictive ability was developed on the basis of pharmacophore hypothesis with $R^2 = 0.97$, $Q^2 = 0.71$, *Pearson-R* $= 0.94$, and $r^2_{pred} = 0.84$. Besides, visualization of the 3D-QSAR model in the context of the molecules under study affords details of the connection between structure and activity, which clearly indicates the features for designing better analogues. The effects

of H-bond acceptor at positions C-6, N-1″, and C-3″, positively ionizable group at N-1′ position, addition of electron-withdrawing group at C-6 and N-3′ was identified as an important criteria and vital regions for substitution of febrifugine-based antimalarial compounds. This ligand-based 3D-QSAR model could be very useful for virtual screening and lead optimization for the identification and development of better molecule against chloroquine-resistant strains of *P. falciparum*.

ACKNOWLEDGMENT

REFERENCES

1. Kuehl FA Jr, Spencer CF, Folkers K. Alkaloids of Dichroa Febrifuga Lour. J Am Chem Soc 1948;70:2091-3.

2. Koepfli JB, Mead JF, Brockman JA Jr. Alkaloids of Dichroa febrifuga. Isolation and Degradative Studies. J Am Chem Soc 1949;71:1048-54.

3. Murata K, Takano F, Fushiya S, Oshima Y. Enhancement of NO Production in Activated Macrophages in Vivo by an Antimalarial Crude Drug, Dichroa febrifuga. J Nat Prod 1998;61:729-33.

4. Harayama T, Takeuchi. Synthesis of febrifugine derivatives and a solution to the puzzle of the structural determination of febrifugine. Tetrahedron 2003;59:1639-46.

5. Redginal I, Hewitt IR, Wallace WS, Gill ER, Williams JH. An Antimalarial alkaloid from hydrangea: XIII. The effects of various synthetic quinazolones against plasmodium lophurae in ducks. Am J Trop Med Hyg 1952;1:768-77.

6. Fishman M, Cruickshank PA. Febrifugine antimalarial agents. Pyridine analogs of febrifugine. J Med Chem 1970;13:155-6.

7. Chien PL, Cheng CC. Structural modification of febrifugine. Some methylenedioxy analogs. J Med Chem 1970;13:867-70.

8. Kikuchi H, Tasaka H, Hirai S, Takaya Y, Iwabuchi Y, Ooi H, *et al*. Potent febrifugine analogues against the Plasmodium malaria Parasite. J Med Chem 2002;45:2563-70.

9. Takaya Y, Tasaka H, Chiba T, Uwai K, Tanitsu M, Kim HS, *et al*. New type of Febrifugine Analogus, Bearing a Quinolizidine Moiety, Show Potent Antimalarial Activity against palasmodium malaria parasite. J Med Chem 1999;42:3163-6.

10. Hirai S, Kikuchi H, Tasaka HS, Begum K, Wataya Y, Tasaka H, *et al*. Metabolite of febrifugine and its synthetic analogue by mouse liver S9 and their antimalarial activity against plasmodium malaria parasite. J Med Chem 2003;46:4351-9.

11. Dei-Cas E, Slomianny C, Charet P, Prensier G, Ajana F, Ramage C, *et al*. In vitro growth and chloroquine sensitivity of Plasmodium falciparum (FCR-3 strain) in red blood cells containing HbC. Parasitol Res 1987;73:306-12.

12. Chen IJ, Foloppe N. Drug-like Bioactive structures and conformational coverage with the LigPrep/ConfGen Suite: Comparison to programs MOE and catalyst. J Chem Inf Model 2010;50:822-39.

13. Yazal JE, Prendergast FG, Shaw DE, Pang YP. Protonation states of the chromophore of denatured green fluorescent proteins predicted by ab initio calculations. J Am Chem Soc 2000;122:11411-5.

14. Schneebeli ST, Hall ML, Breslow R, Friesner R. Quantitative DFT modeling of the enantiomeric excess for dioxirane-catalyzed epoxidations. J Am Chem Soc 2009;131:3965-73.

15. Mehdipour AR, Safarpour MA, Taghavi F, Jamali M. Density functional theory-based Quantitative Structure Activity Relationship (QSAR) study of alkanol and alkanthiol derivatives. QSAR Combi Sci 2009;28:568-75.

16. Deeb O, Clare BW. Comparison of AM1 and B3LYP-DFT for Inhibition of MAO-A by Phenylisopropylamines: A QSAR Study. Chem Biol Drug Des 2008;71:352-62.

17. Dixon SL, Smondyrev AM, Rao SN. PHASE: A novel approach to pharmacophore modeling and 3D database searching. Chem Biol Drug Des 2006;67:370-2.

18. Evans AA, Doman TN, Thorner DA, Bodkin MJ. 3D QSAR methods: Phase and catalyst compared. J Chem Inf Model 2007;47:1248-57.

19. Narkhede SS, Degani MS. Pharmacophore Refinement and 3D-QSAR Studies of Histamine H3 Antagonists. QSAR Comb Sci 2007;26:744-53.

20. Watts KS, Dalal P, Murphy RB, Sherman W, Friesner RA, Shelley JC. Conf gen: A conformational search method for efficient generation of bioactive conformers. J Chem Inf Model 2010;50:534-46.

21. Tawari NR, Bag S, Degani MS. Pharmacophore mapping of a series of pyrrolopyrimidines, indolopyrimidines and their congeners as multidrug resistance-associated protein (MRP1) modulators. J Mol Model 2008;14:911-21.

22. Gmiz-Hernndez AP, Artur S. Galstyan, Knapp EW. Understanding Rubredoxin redox potentials: Role of H-bonds on model complexes. J Chem Theory Comput 2009;5:2898-908.

23. Wold S, Geladi P, Esbensen K, Öhman J. Multi-way principal components-and PLS-analysis. J Chemom 1987;1:41-56.

24. Li Y, Wang Y, Zhang F. Pharmacophore modeling and 3D-QSAR analysis of phosphoinositide 3-kinase p110α inhibitors. J Mol Model 2010;16:1449-60.

New features on the journal's website

Optimized content for mobile and hand-held devices
HTML pages have been optimized of mobile and other hand-held devices (such as iPad, Kindle, iPod) for faster browsing speed.
Click on **[Mobile Full text]** from Table of Contents page.
This is simple HTML version for faster download on mobiles (if viewed on desktop, it will be automatically redirected to full HTML version)

E-Pub for hand-held devices
EPUB is an open e-book standard recommended by The International Digital Publishing Forum which is designed for reflowable content i.e. the text display can be optimized for a particular display device.
Click on **[EPub]** from Table of Contents page.
There are various e-Pub readers such as for Windows: Digital Editions, OS X: Calibre/Bookworm, iPhone/iPod Touch/iPad: Stanza, and Linux: Calibre/Bookworm.

E-Book for desktop
One can also see the entire issue as printed here in a 'flip book' version on desktops.
Links are available from Current Issue as well as Archives pages.
Click on View as eBook